

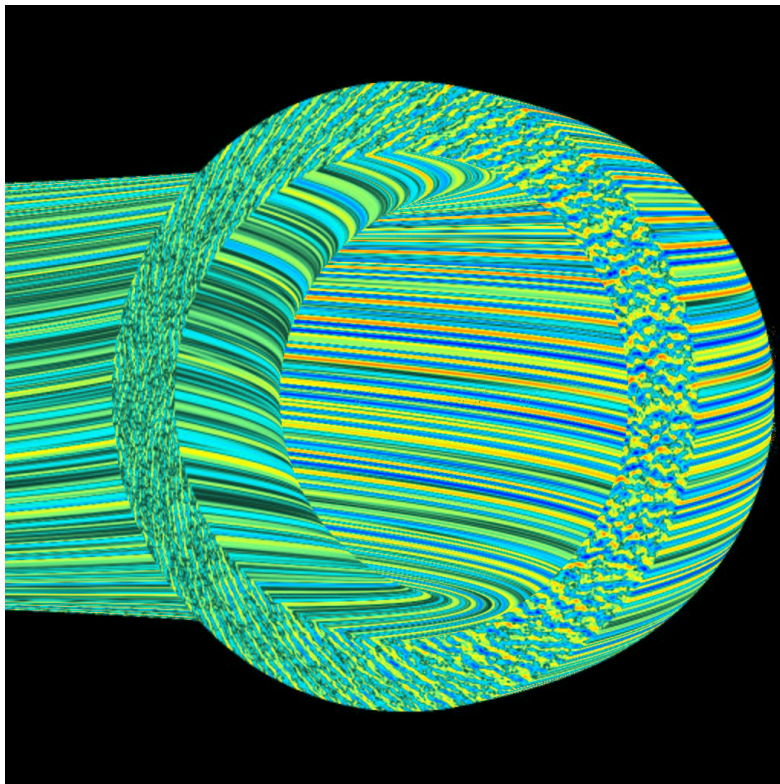
Gyrokinetics at Imperial College

W Dorland, Imperial College

Collabs: Rogers, Jenko, Kotschenreuther, Hammett, Cowley

Joint European Torus

26 Nov, 2001



Overview

1. Gyrokinetic equations
2. General geometry, simulation domain
3. Microinstability basics: linear
4. ETG turbulence
5. Zonal flow dynamics
6. Dimits shift (nonlinear instability threshold)
7. Dominant role of collisions
8. Opportunities

Gyrokinetic Equation

- Gyrokinetic equation appropriate if

$$\frac{\omega}{\Omega} \sim \frac{k_{\parallel}}{k_{\perp}} \sim \frac{\delta f}{f} \sim \frac{e\delta\Phi}{T} \sim \frac{\delta B}{B} \sim \frac{\rho}{L} \ll 1$$

- Gyrokinetic equation describes evolution of perturbed distribution function $h = h_s(\rho, \alpha, \theta, \epsilon, \mu; t)$. For $F_0 = F_0(\epsilon, \Psi)$:

$$\left(\frac{d}{dt} + v_{\parallel} \hat{\mathbf{b}} \cdot \nabla + i\omega_d + C \right) h = i\omega_*^T \chi - q \frac{\partial F_0}{\partial \epsilon} \frac{\partial \chi}{\partial t}.$$

- The total derivative is

$$\frac{dh}{dt} = \frac{\partial h}{\partial t} + \frac{c}{B} \{ \chi, h \}.$$

- The drift frequency $i\omega_*^T = n_0 c \partial F_0 / \partial \Psi$, where n_0 is the toroidal mode number of the perturbation and Ψ is the equilibrium poloidal magnetic flux enclosed by the magnetic surface of interest.
- The perpendicular drifts (curvature, grad-B) are

$$\omega_d = \mathbf{k}_{\perp} \cdot \mathbf{B}_0 \times \left(m v_{\parallel}^2 \hat{\mathbf{b}} \cdot \nabla \hat{\mathbf{b}} + \mu \nabla B_0 \right) / (m B_0 \Omega),$$

- The fields are represented by

$$\chi = J_0(\gamma) \left(\Phi - \frac{v_{\parallel}}{c} A_{\parallel} \right) + \frac{J_1(\gamma)}{\gamma} \frac{m v_{\perp}^2}{q} \frac{\delta B_{\parallel}}{B}.$$

Here, $\gamma = k_{\perp} v_{\perp} / \Omega$.

Gyrokinetic Maxwell Equations

- Fields determined by Maxwell equations, neglecting displacement current.
- Poisson's equation:

$$\nabla_{\perp}^2 \Phi = 4\pi \sum_s \int d^3v q \left[q\Phi \frac{\partial F_0}{\partial \epsilon} + h \exp(iL) \right],$$

where $L = (\mathbf{v} \times \hat{\mathbf{b}} \cdot \mathbf{k}_{\perp})/\Omega$ accounts for the gyrophase dependence.

- Preferred velocity space coordinates are (ϵ, μ, ξ) , so that

$$\int d^3v = \frac{B}{m^2} \int \frac{d\epsilon d\mu d\xi}{|v_{\parallel}|} \equiv \frac{1}{2\pi} \int d^2v d\xi$$

- Integrate over the gyrophase to find

$$\nabla_{\perp}^2 \Phi = 4\pi \sum_s \int d^2v q \left[q\Phi \frac{\partial F_0}{\partial \epsilon} + J_0(\gamma)h \right]$$

- Similarly, Ampere's equation provides the two components of the perturbed magnetic field:

$$\nabla_{\perp}^2 A_{\parallel} = -\frac{4\pi}{c} \sum_s \int d^2v q v_{\parallel} J_0(\gamma)h$$

$$\frac{\delta B_{\parallel}}{B} = -\frac{4\pi}{B^2} \sum_s \int d^2v m v_{\perp}^2 \frac{J_1(\gamma)}{\gamma} h$$

General Geometry

- Metric coefficients for general geometry calculations are well known. Given a Clebsch representation of the magnetic field:

$$\mathbf{B} = \nabla\alpha \times \nabla\psi$$

one can calculate all needed quantities.

- In the field-line-following (ballooning) limit, perturbed quantities are represented by

$$A = \hat{A}(\theta) \exp(iS)$$

where $\hat{\mathbf{b}} \cdot \nabla S = 0$. This takes into account the fact that the perturbations tend to be slowly varying along the field line, and allows for rapid variation across the field line.

- To make contact with the ballooning approximation and with field-line following coordinates, choose

$$S = n_0 (\alpha + q\theta_0),$$

where n_0 is an integer, θ_0 is the ballooning parameter, $q(\Psi) = d\Psi_T/d\Psi$, $\Psi_T = (2\pi)^{-2} \int_V d\tau \mathbf{B} \cdot \nabla\phi$ is the toroidal flux, and $d\tau$ is the volume element.

- Simulation coordinates are therefore (Ψ, α, θ) .

Flux-Tube Simulation Domain

We use field-line-following coordinates in a “flux-tube.”

- Simulation domain has a “small” perpendicular cross-section:
The simulation domain should be at least a few turbulent correlation lengths long in each direction.
- The variation of the gradient scale lengths across the simulation domain is assumed to be small.
- The energy, momentum and/or particle sources and sinks inside the flux-tube are assumed to be small.
- Radial periodicity prevents artificial flattening of driving gradients.
- Non-trivial periodicity condition along the field line makes field-line-following coordinates exactly equivalent to ballooning transformation when parallel correlation length

$$\lambda_{\parallel} < 2\pi qR.$$

- For small ρ/a , flux tube assumptions reduce the total simulation volume significantly.

Summary of Numerical Issues: GS2

- Electrostatic and electromagnetic perturbations treated on equal footing.
- 5-D distribution function $h = h_s(\Psi, \alpha, \theta, \epsilon, \mu; t)$ evolved in time for each species.
- **Implicit integration** of fast motion along field lines reduces time step restrictions and automatically **recovers appropriate orbit averages**, without any subsidiary ordering of nonlinear terms.
- Velocity-space filamentation not a problem for realistic collision frequencies with **full Lorentz collision operator**.
- GS2 uses spectral decomposition in the two directions perpendicular to the field line and for energy and pitch angle for good accuracy with minimal memory & CPU usage.
- Pseudo-spectral evaluation of nonlinear terms is fast, without introducing numerical dissipation.
- Flux-tube simulation domain is maximally consistent with GK ordering.
- Source code available on-line; presently 18 users.

Microinstability Basics: Linear

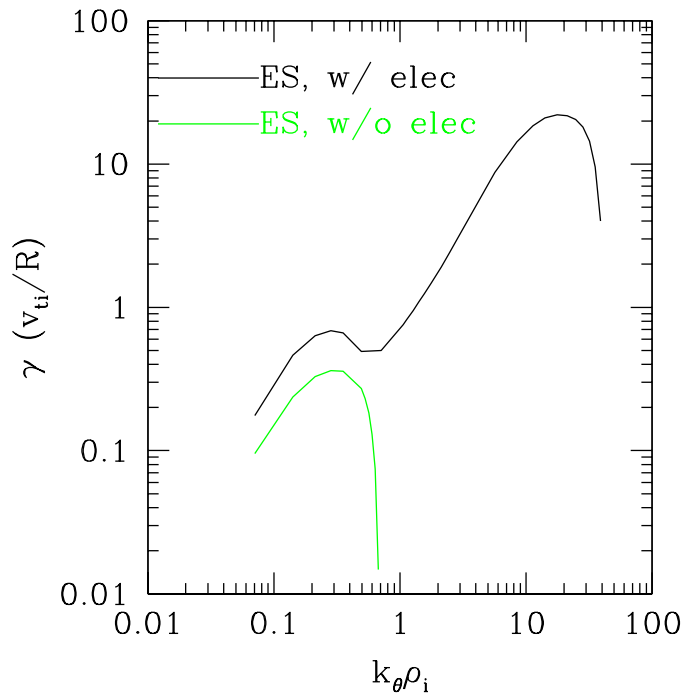
- Instabilities driven by gradients in temperature, momentum and/or density.
- Growth rates typically proportional to ω_* , wavelengths typically several gyro-radii.
- In core plasma, three most important instabilities are:
 1. **ITG**, driven by **I**on **T**emperature **G**radient;
 2. **TEM** (**T**rapped **E**lectron **M**ode) driven mainly by density gradients;
 3. **ETG**, driven by **E**lectron **T**emperature **G**radient;
- Linear properties well-understood theoretically, but realistic assessment of stability requires state-of-the-art calculation since typically $k_{\perp}\rho \sim 1$,

$$\omega \sim k_{\parallel} v_t, \quad \omega_d, \quad \omega_b$$

multiple gradients co-exist, and geometric effects (magnetic shear, shaping, *etc.*) are strong.

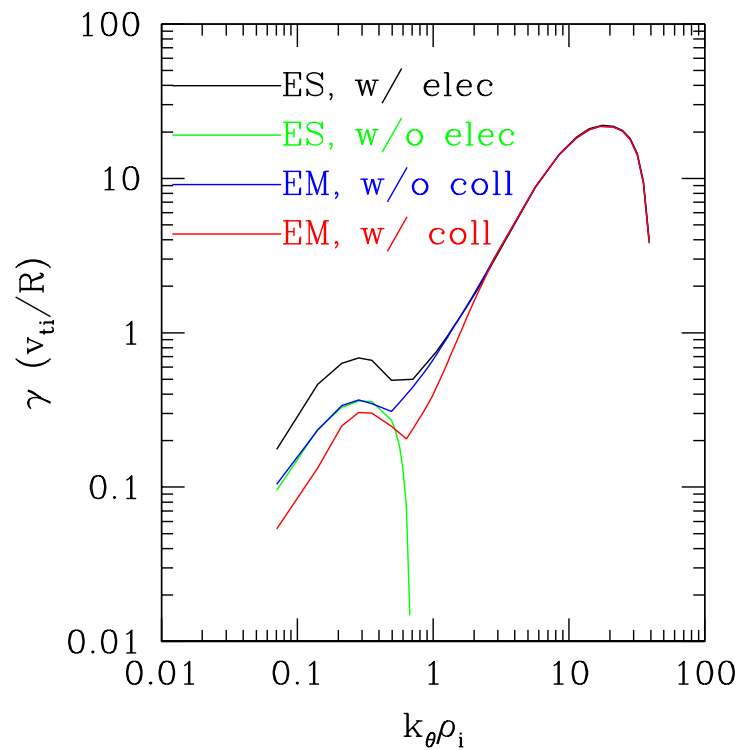
Electron Dynamics Enhances Instability

- Early simulations assumed electron response was adiabatic. Allowed reasonable assessment of ITG-induced energy transport.
- To understand particle and electron energy transport, electron dynamics must be included.
- Trapped electrons enhance long wavelength instabilities; influence reduced by collisions. Passing electrons enable ETG modes.



Electron Dynamics Introduces Electromagnetic Turbulence

- Passing electrons carry perturbed currents, which may introduce small scale magnetic islands, but which also modestly stabilize ITG modes.
- Possibility of magnetic electron energy transport exists.
- Toroidal ETG modes linearly unaffected by finite β .



ETG Modes Often Ignored Because Mixing Length Transport is Small

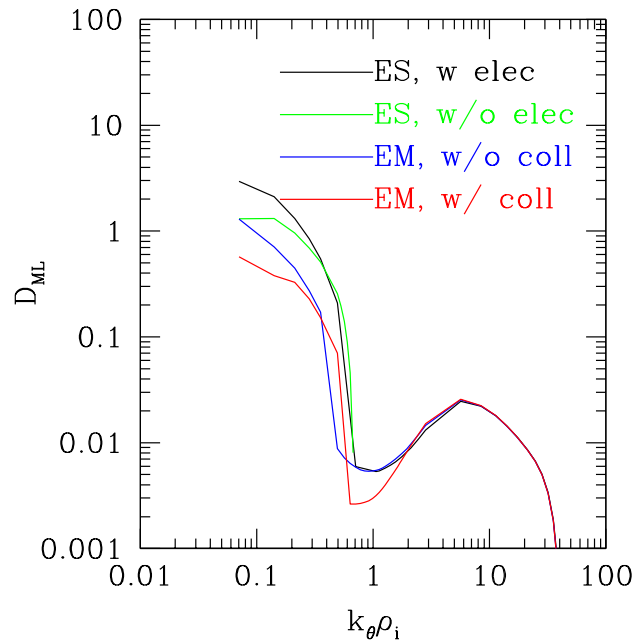
- Mixing length estimate of transport is

$$D_{\text{ML}} \sim \frac{\gamma}{\bar{k}_{\perp}^2}$$

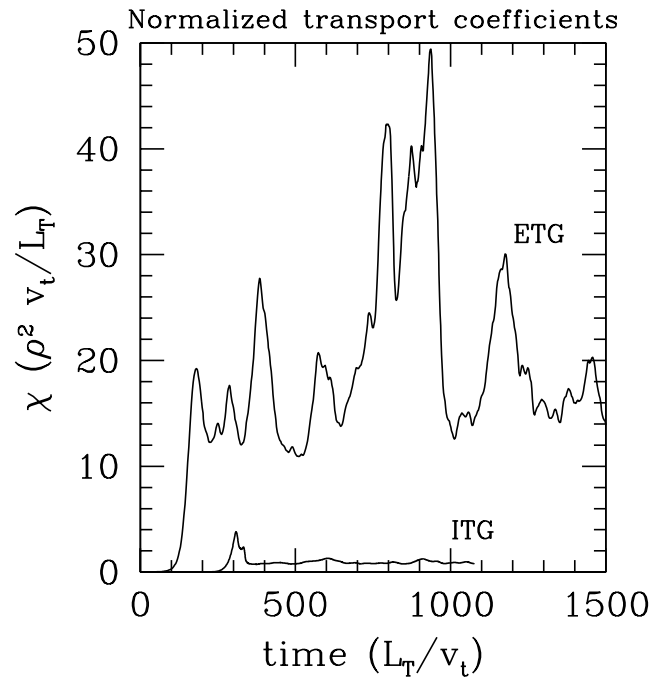
where γ is the linear growth rate. Results from balance of linear and nonlinear terms:

$$\frac{\partial h}{\partial t} + \frac{c}{B} \{\chi, h\} + v_{\parallel} \hat{\mathbf{b}} \cdot \nabla h + i\omega_d h + Ch = i\omega_*^T \chi - q \frac{\partial F_0}{\partial \epsilon} \frac{\partial \chi}{\partial t}$$

- Because $\gamma \sim \omega_*$, this decreases at high k_{\perp} .



Nonlinear ETG Simulations Show Transport Larger than Mixing Length



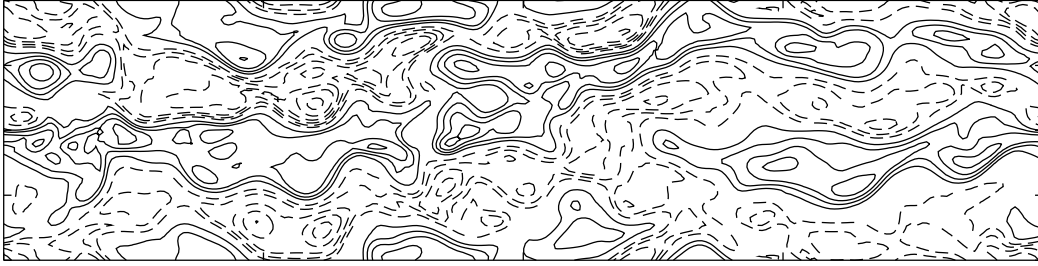
- ETG and ITG mixing length expectation:

$$\frac{\chi_e^{\text{ETG}}}{\rho_e^2 v_{te} / L_{Te}} \sim \frac{\chi_i^{\text{ITG}}}{\rho_i^2 v_{ti} / L_{Ti}}$$

so that $\chi_e^{\text{ETG}} / \chi_i^{\text{ITG}} \sim \sqrt{m_e / m_i} \sim 1/60$

- EM GK simulations show that “streamers” can lead to large *normalized* ETG transport coefficients, so that $\chi_e^{\text{ETG}} \sim \chi_i^{\text{ITG}}$
- Occurs because secondary instabilities that produce saturation are weak in the ETG limit

Radially Elongated Streamers Found in ETG Simulations



- Governing equation is

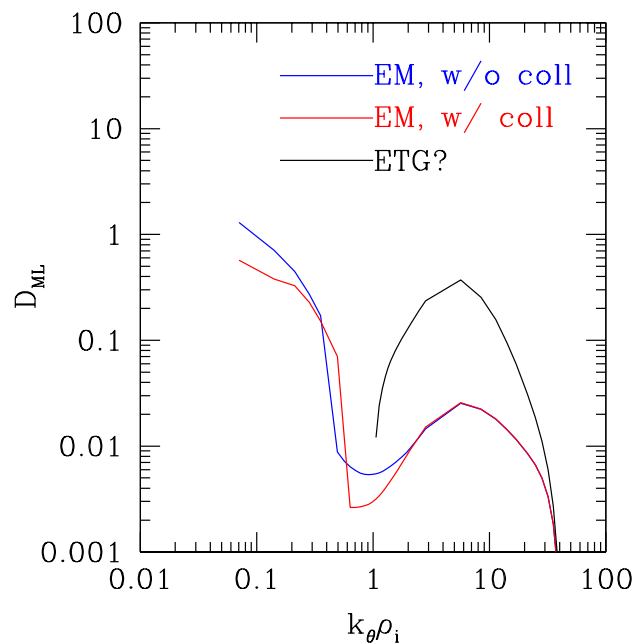
$$\left[\left(\frac{\tau}{1+\tau} \right) \gamma + k_x^2 \bar{\gamma} \right] \tilde{\psi} = \partial_y \left[\bar{\gamma}^2 \partial_y (\tilde{\psi} / \bar{\gamma}) \right]$$

with $\bar{\gamma} = \gamma - ik_x \psi'_p(y)$ and $\tau = Z_{\text{eff}} T_e / T_i$.

- Here, ψ_p is the guiding center electrostatic potential from ETG eigenmode.
- Instability differs from conventional Kelvin-Helmholtz (KH) because of the **first term on the left-hand side (the ion response)**.
- Balancing ion response with the other terms leads to a maximum growth rate $\sim k_p^4 \psi_{p0}$ for $k_x \sim k_p$.
- This is weaker than conventional KH by a factor of $(k_\perp \rho_e)^2$, and still weaker compared to ITG secondary instabilities.

ETG Modes Likely Contribute to Electron Energy Transport

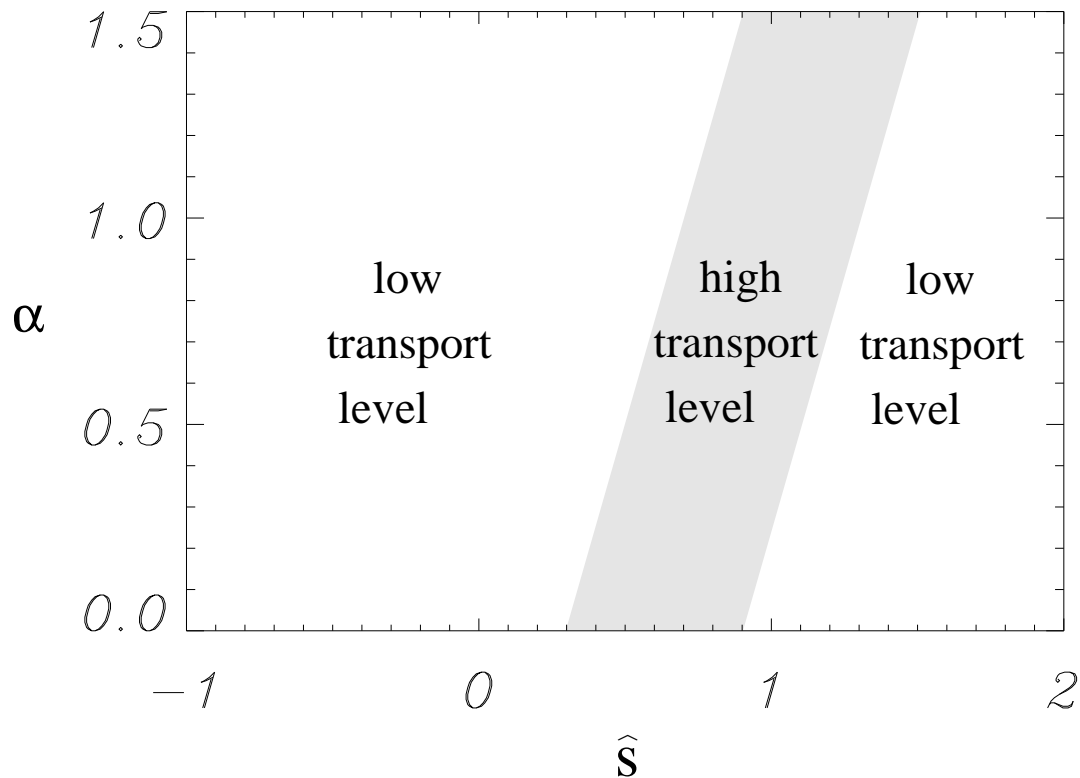
- Because $k_{\perp}\rho_i \gg 1$, one does not expect (or find) significant particle or ion energy transport.
- Simple expectation from secondary stability saturation mechanism:



- However, mysteries remain. Preliminary evidence suggests ETG $\chi_e \sim 1/\beta$ in some regimes. Important for Ohmic core? Pedestal? ITB?
- Very hard to stabilize ETG modes with velocity shear. More interesting *second microstability* possibilities exist.

Strongly Reversed Magnetic Shear Can Reduce ETG Transport

- For typical core gradients, approximately 25 nonlinear runs used to map out suggestive diagram:



- For steeper gradients (such as may be found in ITB's) the high transport region extends to negative magnetic shear.
- Strongly reversed magnetic shear should reduce electron energy transport in ITB. Feedback loop possible?

For Modes with $k_{\perp}\rho_i < 1$, Secondary Instabilities are Strong

- Governing equation is

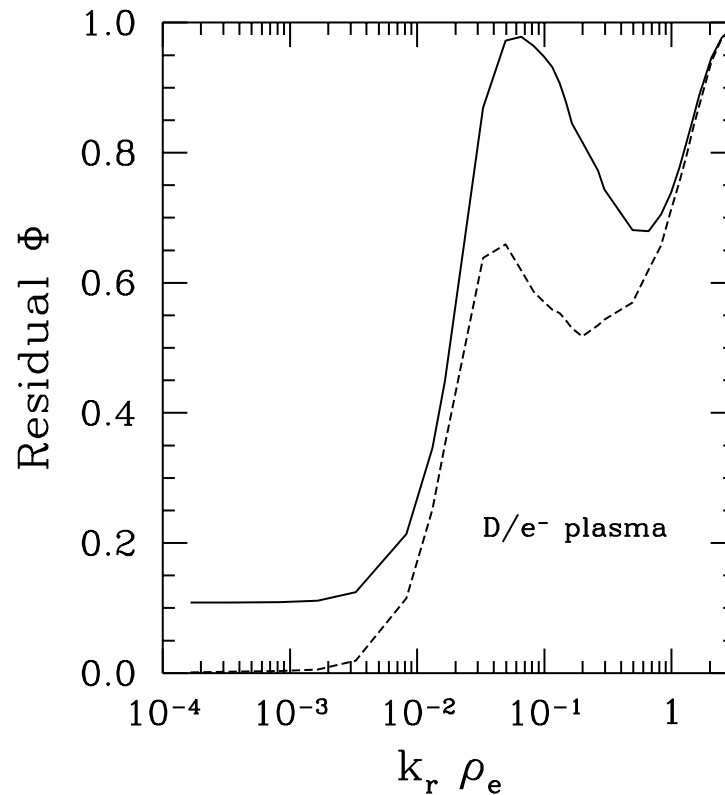
$$-(1 + \tau k_x^2)\bar{\gamma}\langle\tilde{\psi}\rangle + [\gamma + k_x^2\Gamma]\tilde{\psi} = \partial_y \left[\bar{\gamma}\partial_y(\tilde{\psi}/\bar{\gamma}) \right]$$

with $\tau = T_i/T_e$, $\Gamma = \tau\gamma + \bar{\gamma}T$ and

$$\bar{\gamma} = \gamma - ik_x\psi_l'(y), \quad \bar{\gamma}T = \gamma - ik_x[(1 + \tau)\psi_l'(y) + \tau T_l'(y)].$$

- Here, ψ_l and T_l are the guiding center electrostatic potential and temperature from an ITG eigenmode.
- Instability differs from conventional Kelvin-Helmholtz (KH) mainly because of the **first two terms on the left-hand side (the electron response)**.
- First term leads to enhancement of instability by a factor $1/(k_{\perp}\rho_i)$.
- As a result, secondary instabilities in ITG limit are strong, driving zonal flows robustly.

Rosenbluth and Hinton: Linearly Undamped Zonal Flows Exist



- Dielectric shielding of static component of driven zonal flow is incomplete. At long wavelengths, trapped ions adjust to permit linearly undamped zonal flows in collisionless limit.
- Lower (dashed) curve has $r/R = 0$. Upper (solid) curve has $r/R = 0.18$.
- **Puzzle: Dielectric shielding decreases at short wavelength. Why isn't ETG transport negligible?**

Tertiary Instabilities Control Zonal Flow

- Zonal flows driven strongly by ITG secondaries, weakly by ETG secondaries.
- Zonal flows themselves weakly unstable at long wavelength, strongly unstable at sub- ρ_i scales.
- At long wavelengths, governing equation is

$$\begin{aligned} & [(1 + (1 + \tau)k_x^2)\bar{\gamma} + ik_y(k_y^2\tau T'_0 - \tau\psi_0''')] \tilde{\psi} \\ & = \partial_x \left[(\tau\gamma + \bar{\gamma}_T)\bar{\gamma}\partial_x(\tilde{\psi}/\bar{\gamma}) \right] \end{aligned}$$

with

$$\bar{\gamma} = \gamma + ik_y\psi'_0(x), \quad \bar{\gamma}_T = \gamma + ik_y[(1 + \tau)\psi'_0(x) + \tau T'_0(x)]$$

- Here, ψ_0 and T_0 are the guiding center electrostatic potential and temperature from zonal flow.
- Natural scale of eigenmode which is localized at x_0 is

$$\lambda = (2\tau T'_0/\psi_0''')^{1/4}|_{x_0}$$

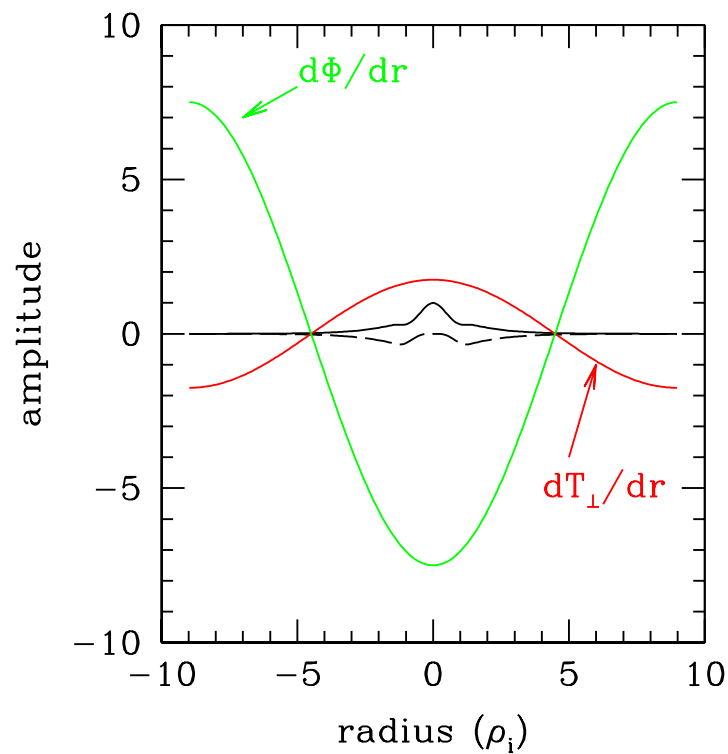
- Ignoring background gradients, maximum (over k_y) growth rate of instability is

$$\gamma \simeq 0.55k_y\sqrt{\tau T'_0\psi_0'''/2}$$

in good agreement with the simulations.

Tertiary Instability Driven by Combination of Gradients Inherent to RH Flows

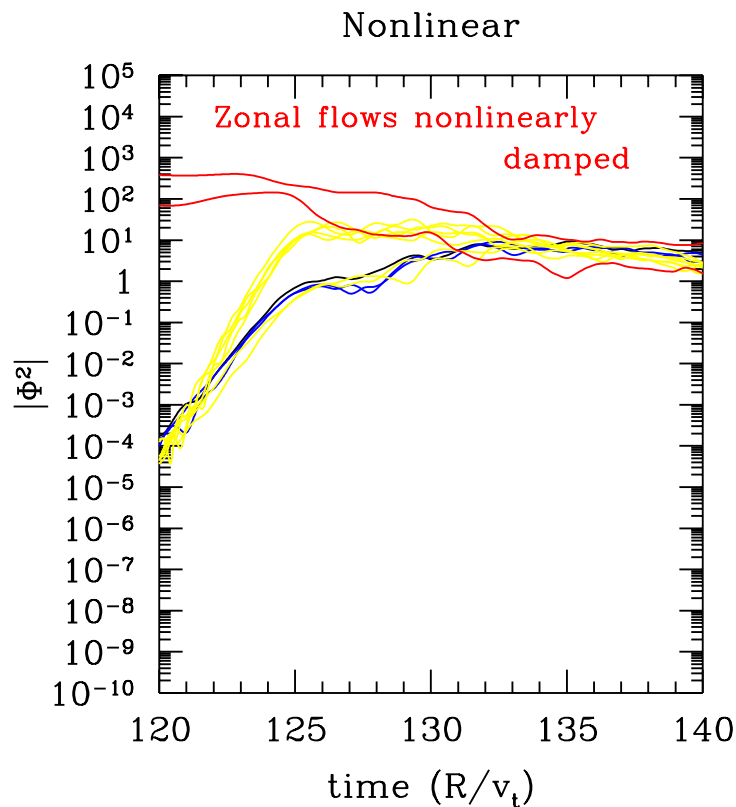
- Example calculation for typical parameters.
- T_{\perp} and Φ perturbations easily shown to be out of phase for Rosenbluth-Hinton zonal flows.



- Precise stability threshold determined by including magnetic shear, curvature, *etc.* is complicated. **In general, weak zonal flows are stable.**

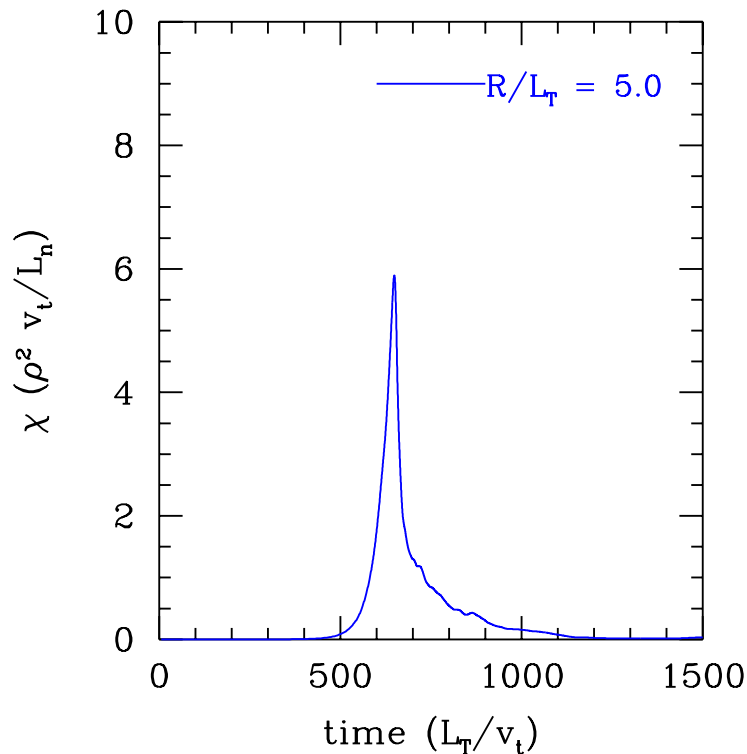
Tertiary Instability Damps Zonal Flows

- Numerical test required to determine whether this instability is strong enough to regulate zonal flows.
- Initialized zonal flows (red) at high amplitude, all other Fourier modes at low level. No equilibrium gradients. Without tertiary instability, these flows are undamped.
- Tertiary modes (yellow) grow at expected rate, observed to break up zonal flows.



At Long Wavelengths, It Is Possible to Quench Turbulence With Self-Generated Zonal Flows

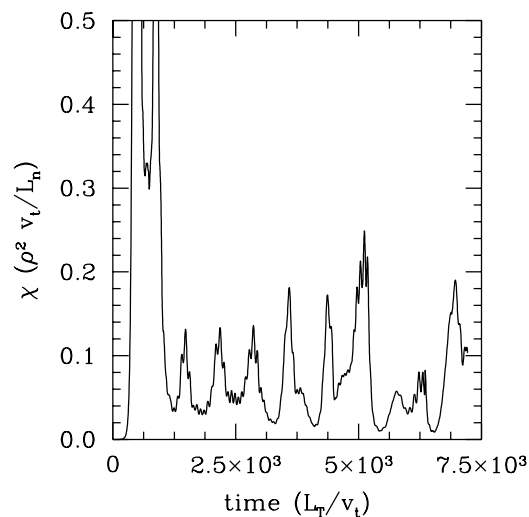
- Consider parameters for which there is linear instability.
- RH zonal flows that are stable to small perturbations may exist. For weakly unstable modes, these RH zonal flows restore linear stability.



The turbulent heat flux quickly falls to zero.

Ion-ion collisions Damp Self-Generated Zonal Flows

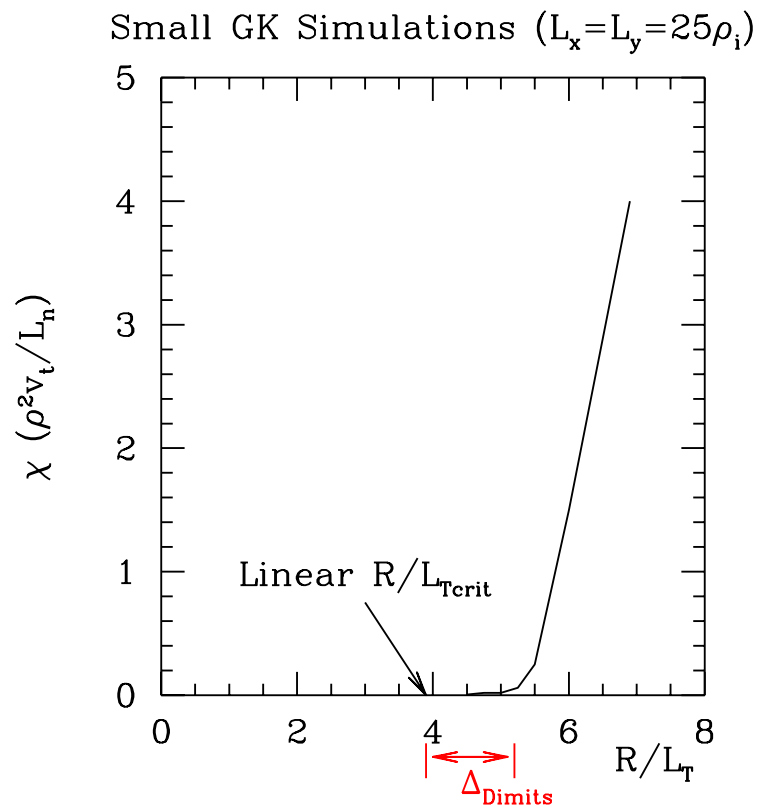
- As pointed out by Rosenbluth and Hinton, and Diamond and Rosenbluth, ion-ion collisions can in principle regulate zonal flows.
- In such a case, increasing temperature would decrease ν_{ii} , allowing the zonal flow amplitude to increase, and therefore reducing the turbulent transport. **Hypothesized to be important in ITER-class tokamak.**
- **Z. Lin, *et al.***, confirmed the role of ion-ion collisions when self-generated RH flows would otherwise restore linear stability. Bursty behaviour observed.
- Here's an example from GS2:



We will return to the role of ν_{ii} later in this talk.

In Such Regimes, Linear Threshold is Basically Irrelevant

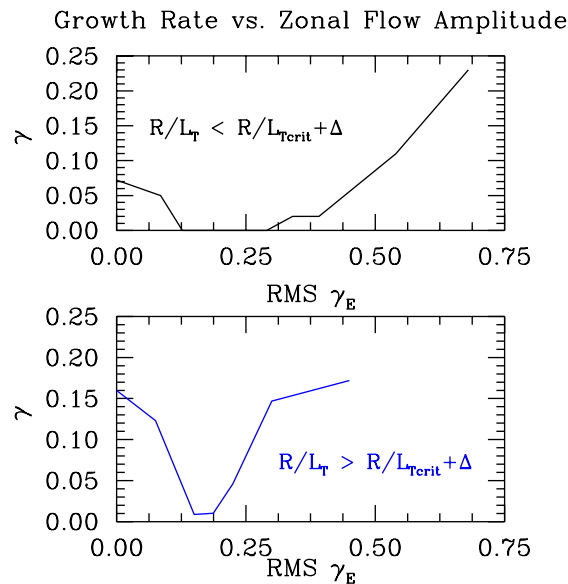
- In collisionless plasma, regime of nonlinearly-upshifted critical gradient for long-wavelength turbulence discovered by [A. Dimits](#).
- Easily reproduced. Model case:



- Important question: What defines this regime? *I.e.*, what limits the Dimits shift?

Dimits Shift Limited by Tertiary Instability

1. Consider several nonlinear simulations for which the spectrum of zonal flows is taken from a nonlinear simulation for which $R/L_T < R/L_{T_{\text{crit}}} + \Delta$ by a small amount.
2. Calculate stability of zonal flows as a function of amplitude of zonal flows. Record linear growth rate when it exists.
3. Repeat calculations, except increase background temperature gradient to be slightly greater than $R/L_{T_{\text{crit}}} + \Delta$.

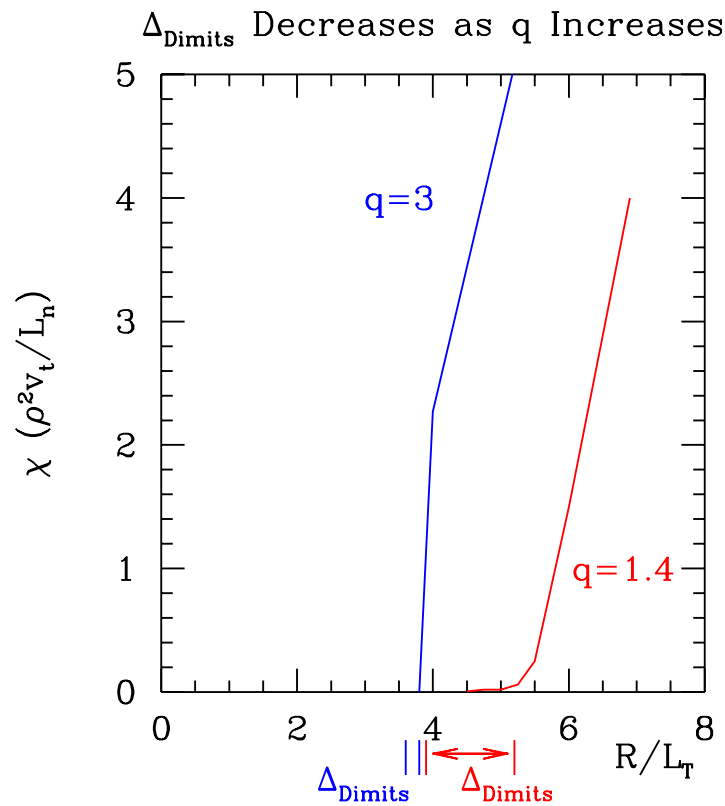


- Tertiary instability threshold corresponds to $R/L_T + \Delta$.

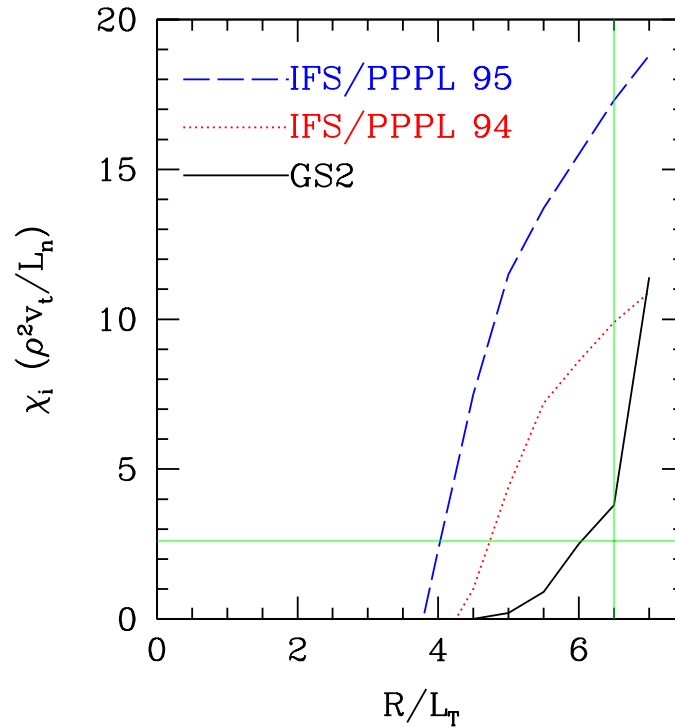
Self-generated zonal flows are regulated by tertiary instability.

Tertiary Instability Threshold Sensitive to Safety Factor

- Full formula for threshold of tertiary mode remains to be discovered. Numerical tests show magnetic shear and safety factor raise threshold. Example: safety factor.



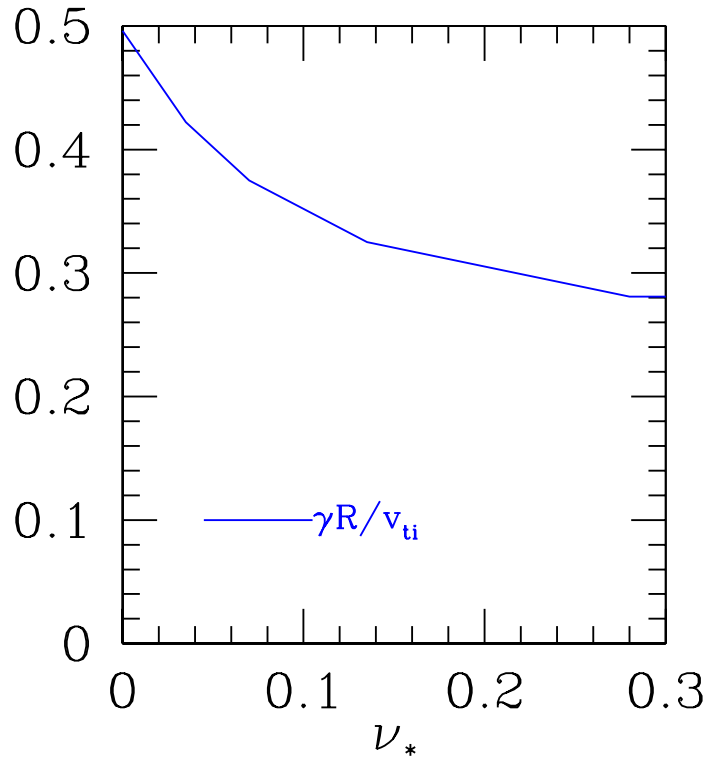
Experimental data consistent with Dimitis shift



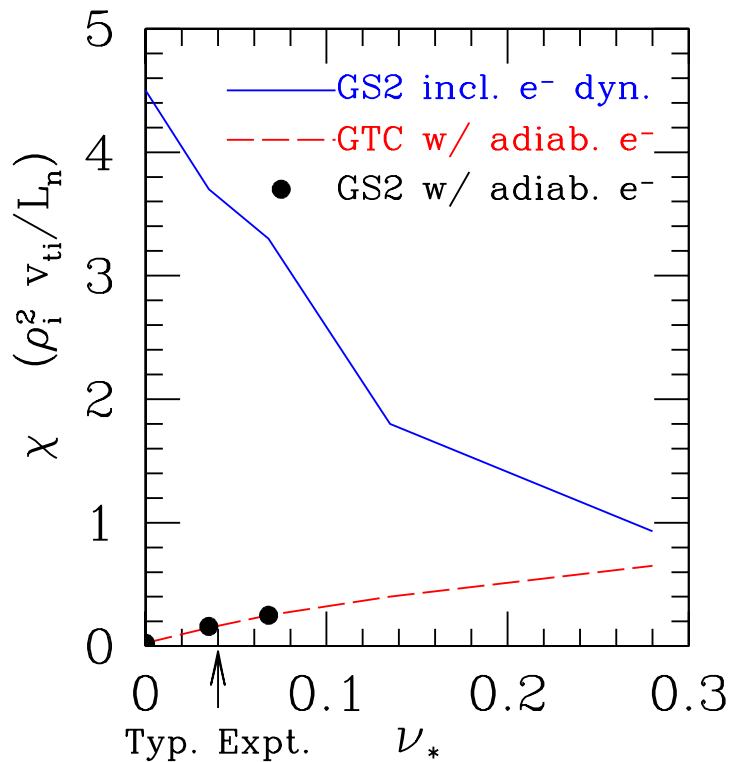
- Comparison with ELMy H-mode from C-Mod; case for which IFS/PPPL models are clearly too high
- Half radius, shot 960116027, $t = 0.9$, $q = 1.3$.
- GS2 simulations with gyrokinetic electrons and ions, collisionality, general geometry
- Nonlinear upshift of R/L_{Tcrit} clearly improves agreement
- Note: Collisions *increase* upshift and *reduce* transport (because non-adiabatic electron response is reduced) – opposite to finding of Lin, Diamond, *et al.*

Collisional reduction of trapped electron response to ITG turbulence

- Lin simulations assumed adiabatic electron response
- Non-adiabatic electron response due to trapped electrons significant at typical core collisionalities
- Non-adiabatic electrons increase ITG growth rate (well-known, ignored by Lin, *et al.*)



Dominant core collisional effect: ν_{ei}



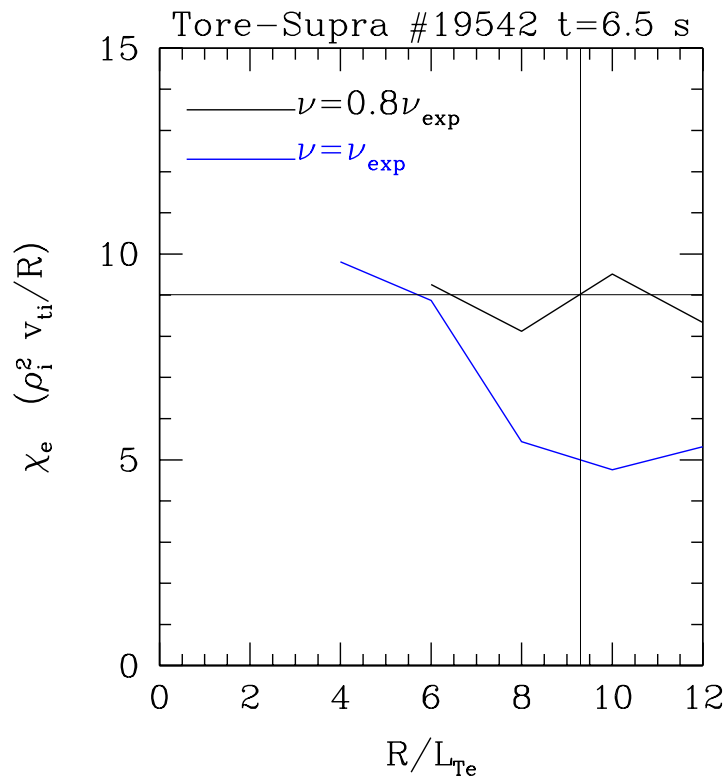
- Cyclone parameters except $R/L_T = 5.3$ and trapped electrons included.
- Increasing collisionality in experimental range of collisionality
- χ strongly *decreases* – zonal flow damping effect is swamped by decrease in non-adiabatic electron response.

Importance of Dimits Shift for Tokamak Performance

- Dimits shift may be important for understanding cases for which core ion temperature profiles are experimentally determined to be **stiff**, even though the gradient **exceeds** the linear threshold of the ITG mode. Because of the strong safety factor scaling, this is probably important mainly at high current.
- Known dependences are not consistent with a strong role for stable, self-generated, zonal flows in barrier formation. However, this remains an open subject of substantial interest.
- To the extent that this effect is important, it scales poorly for larger, hotter tokamaks, because of the destabilization associated with non-adiabatic electron dynamics at low collisionality.
- Other questions: Is there an anti-Dimits shift? Is the pedestal width in fact determined by the stability of the pedestal flows to the tertiary instability?

Opportunities for Focus: Electron Energy Transport

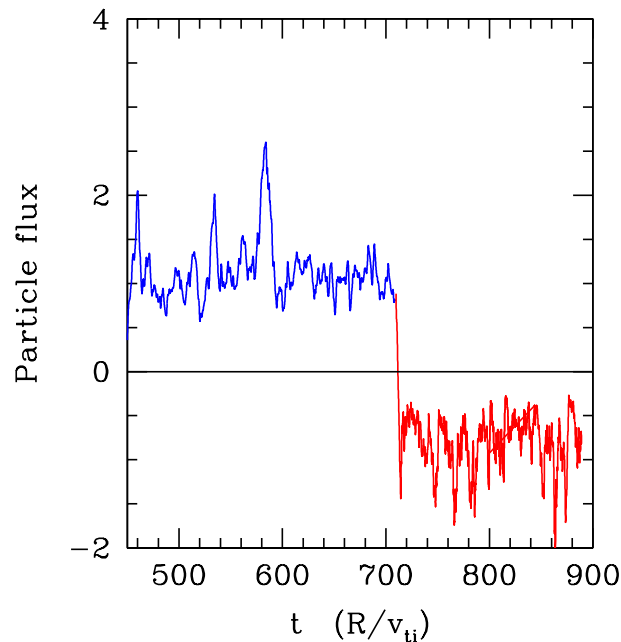
- Experimental tests of transport channels other than ion energy transport needed.
- Tore Supra has excellent data for electron energy transport with which we are comparing. Example:



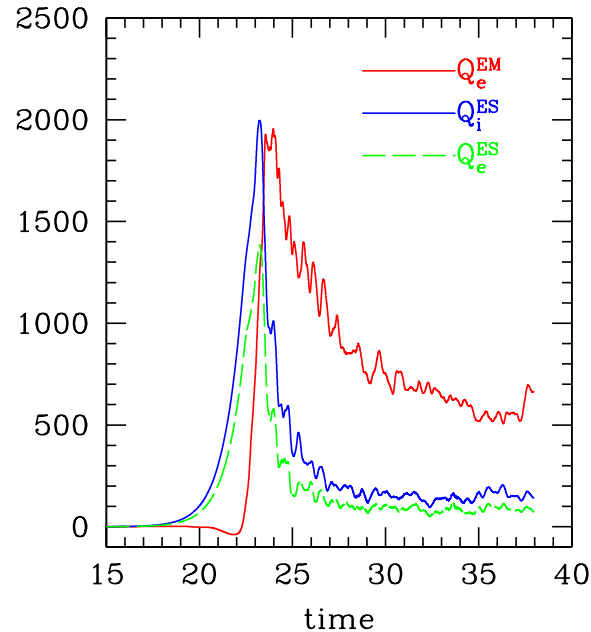
- This is a case for which the ions are cold. Note the unusual behaviour of χ_e vs. R/L_{Te} .

Opportunities for Focus: Particle Transport

- Simulations predict an anomalous inward flux of particles – up the gradient. A careful experimental test of this prediction would be interesting.
- Core parameters are taken from Tore Supra. Shown is the turbulent particle flux *vs.* time from a nonlinear simulation.
- At $\tau=700$, the ion temperature gradient is increased slightly, and the particle flux is observed to reverse, despite the presence of a substantial density gradient.



Opportunities for Focus: Magnetic Transport



- As β approaches the ideal ballooning limit β_c , character of ITG turbulence changes
- Energy transport dominated by

$$Q_e^{EM} \sim \langle q_{\parallel} \delta B_{\perp} / B_0 \rangle$$

- EM particle transport is negligible
- Occurs when finite k_{θ} component of secondary instability has significant EM component
- Experimentally testable?

Summary

- Gyrokinetic simulations are a new tool with value.
- Progress has been made in understanding which instabilities are important, their relevant threshold criteria, and the dynamics of nonlinear saturation in different scenarios and regimes.
- Stronger ties to an experimental program are needed to make further progress.
- Quirky simulation results may suggest good experimental tests, needed for further acceptance of the basic approach.
- Imperial College is a leader in this area. No other research group has a toroidal gyrokinetic turbulence code that includes electromagnetic perturbations or general geometry, and Imperial is presently at least one year ahead of the nearest competitor in studying non-adiabatic electron dynamics.